NASA TECHNICAL MEMORANDUM

NASA TM X-52784

NASA TM X-52784

FLIGHT PERFORMANCE OF AUXILIARY INLET EJECTOR AND PLUG NOZZLE AT TRANSONIC SPEEDS

by Nick E. Samanich and Richard R. Burley
Lewis Research Center
Cleveland, Ohio

TECHNICAL PAPER proposed for presentation at
Sixth Propulsion Joint Specialist Conference sponsored by the
American Institute of Aeronautics and Astronautics
San Diego, California, June 15-19, 1970

FLIGHT PERFORMANCE OF AUXILIARY INLET EJECTOR AND PLUG NOZZLE AT TRANSONIC SPEEDS

by Nick E. Samanich and Richard R. Burley

Lewis Research Center
Cleveland, Ohio

TECHNICAL PAPER proposed for presentation at
Sixth Propulsion Joint Specialist Conference sponsored by
the American Institute of Aeronautics and Astronautics
San Diego, California, June 15-19, 1970

NATIONAL AERONAUTICS AND SPACE ADMINISTRATION

FLIGHT PERFORMANCE OF AUXILIARY INLET EJECTOR AND PLUG NOZZLE AT TRANSONIC SPEEDS

Nick E. Samanich and Richard R. Burley
Lewis Research Center
National Aeronautics and Space Administration
Cleveland, Ohio

E-5636

Abstract

Nozzle performance may be sensitive to the type of airframe-nozzle installation. An installation that is of general interest is a podded engine mounted near the aft lower surface of the wing. The effect of this installation on nozzle performance in the transonic speed range is currently being investigated at the Lewis Research Center using a modified F-106B aircraft. This paper will discuss some of the significant results obtained with two of these nozzle types: auxiliary inlet ejector and conical plug. Both of them approximate subsonic cruise geometries of nozzles designed for efficient operation in the Mach 2.8 range.

Introduction

The performance of nozzles for supersonic aircraft may be sensitive to the manner in which they are installed on the airframe. This is particularly true in the transonic speed range where the nozzle is operating off design and where external flow effects are important. An installation that is of general interest is the podded engine mounted near the aft lower surface of a wing with the exhaust nozzles overhanging the wing-trailing edge. This type of installation shields the inlet from angle-of-attack effects, and might provide favorable interference between the nacelle and wing at supersonic speeds[1]. At high subsonic speeds this particular airframe installation also causes increased pressures on the external surface of the nozzle relative to isolated results[2]. This phenomenon is apparently caused by a recompression resulting from the combination of the basic wing and the reflection and amplification of the nacelle flow field by the wing lower surface. At the high subsonic Mach numbers a terminal shock is created which surrounds the nacelle and moves downstream as Mach number increases. As long as the shock is in the vicinity of the nozzle, the external surface pressures are relatively high. Above Mach 0.95 the shock moves downstream of the nozzle which results in a sharp drop in external pressure level.

The effect of this installation on the performance of complex nozzle systems in the transonic speed range is currently being investigated at the Lewis Research Center using a modified F-106B aircraft[2, 3, 4]. Initial tests were conducted with variable flap ejectors. Isolated results for 15° boattail flaps indicated a significant boattail drag reduction could be obtained by rounding the boattail juncture. Installing the sharp-corner boattail under the wing produced a large reduction in subsonic drag (even lower than that of the rounded isolated boattail) but rounding the juncture then had very little additional effect[2].

Subsequent nozzle types studied in this installation were the auxiliary inlet ejector and the conical plug. The auxiliary inlet ejector nozzle has the potential for achieving the performance associated with the more complex mechanically-actuated variable-geometry designs but at reduced weight. This is due to the principle of self actuation for both the auxiliary inlet doors and the trailing-edge flaps which are positioned by the pressure differential across them. The plug is also attractive because it provides good aerodynamic performance, has a low infrared signature, can operate efficiently over a range of pressure ratios with relatively simple geometry changes, and may be quieter than other nozzle types[5].

Performance of these nozzle types was obtained over a Mach number range from 0.7 to 1.3. For the auxiliary inlet ejector, the trailing-edge flaps were fixed in a position appropriate for subsonic and transonic speeds. Both free-floating and fixed-open auxiliary inlet door configurations were investigated at primary nozzle areas corresponding to minimum and maximum afterburning power settings. With the plug nozzle, variations were made in shroud exit diameter, nacelle shape, and plug length. All the plug assemblies were tested with a primary area corresponding to a military power setting. Static[6, 7] and in-flight investigations of these nozzle types have been completed. Performance has been compared with 0.34-scale isolated cold-flow results obtained in the 8- by 6-Foot Supersonic Wind Tunnel. This paper will present some of the significant results obtained with the auxiliary inlet ejector and conical plug.

Flight Facility

Flight tests were conducted with an F-106B aircraft modified to carry two 25.0-inch (63.5 cm) diameter nacelles at 32-percent semispan outboard locations with the exhaust nozzles overhanging the wing-trailing edge. A photograph of the installation is shown in Fig. 1. The underwing nacelles had normal shock inlets and contained calibrated J85-GE-13 turbojet engines as shown schematically in Fig. 2. One of the engines had a calibrated cylindrical ejector which was used as a reference in the analysis of the propulsive forces. Secondary air to cool the engine and afterburner was supplied from the inlet and controlled at the periphery of the compressor face by a rotary valve. The nacelles were attached to the wing by two hinged links permitting forces parallel to the nacelle axis to be recorded by a load cell located between the links. The load-cell measurement was used in combination with a tare force obtained from the reference nacelle to determine nozzle gross thrust minus drag[3].

Engine airflow was determined from engine calibrations along with in-flight measurements of engine speed

and of pressure and temperature at the compressor face. Calibrations of the secondary flow valve were used with measured valve pressure drop and area to determine secondary airflow. Conditions at the primary nozzle exit were determined knowing airflow, turbine discharge conditions, and fuel flow rates. The exhaust nozzle pressure ratio schedule is shown in Fig. 3. This schedule is representative of power settings from military to maximum afterburning. At Mach 0.9 the pressure ratio was 3.70.

Because the nacelles would interfere with the normal F-106 elevon movement, a section of the elevon immediately above the nacelle was cut out and rigidly fixed to the wing. This rigid section of elevon was modified in the form of a trough for tests of nozzles having auxiliary inlets.

Test Hardware

Auxiliary Inlet Ejector

The auxiliary inlet ejector nozzle is shown in Fig. 4 along with the elevon trough. Details of this nozzle design are described in Ref. 6. The nozzle incorporates a series of 16 auxiliary inlet doors located around the periphery of the external skin ahead of the primary nozzle. The doors were double hinged with a 2 to 1 ratio between the aft and the forward ramp angles. The forward and aft door ramps were the same length. The doors were either in fixed positions or allowed to float under the influence of air loads. The top three doors opened to the trough. Fixed double-hinged doors are shown in the wide-open position (tertiary flow area of 163 in.^{2} (1051 cm^2). The trailing-edge flaps were simulated in the closed position with rigid structure which provided a boattail angle of 15° and an exit diameter of 18.19 in. (46.2 cm). Boattail juncture radius-to-nozzle maximum diameter ratio was 0.5. The primary nozzle effective area was set at nominal values of either 133 in.^{2} (858 cm^2) or 173 in.^{2} (1116 cm^2) corresponding to minimum and maximum afterburning, respectively.

Plug Nozzle

The plug nozzle assembly is shown installed on the aircraft in Fig. 5, and details of its design are presented in Ref. 7. The gas generator for the plug nozzle was a J85-GE-13 turbojet with a modified afterburner can. The variable area nozzle was removed and replaced with a strut-supported fixed-plug nozzle which was attached to the afterburner can with a packing gland slip joint. The same 10° half-angle conical plug body was used for all the assemblies; the apex was located approximately 51 in. (129 cm) aft of the wing-trailing edge. The plug size was the largest possible (fig. 6) consistent with a nacelle diameter of 25.0 in. (63.5 cm), an annular secondary area large enough to permit approximately 12-percent cooling flow and a primary throat area of 110 in.^{2} (710 cm^2). Since the plug surface was uncooled, the engine was limited to non-afterburning operation. With this nozzle type, variation in internal expansion required for efficient operation at high pressure ratios can be accomplished by translation of a cylindrical shroud. The configurations tested simulated retracted shroud positions required for efficient low pressure operation.

The cylindrical nacelle assembly (top of fig. 6) had a 17° half-angle conical primary flap designed to represent a hinged iris-type nozzle operating at its minimum area with a capability of 60-percent area modulation. Secondary cooling air was discharged over the primary flap through an annular passage with a minimum flow area of 46 in.^{2} (297 cm^2). Sections of the plug were removable for testing various plug truncations.

The boattailed nacelle configuration in the middle of Fig. 6 simulated a smaller diameter translating shroud having an exit-to-primary throat area ratio of 3.75 as compared to 4.60 for the cylindrical nacelle assembly. The shroud exit diameter was reduced to 22.63 in. (57.5 cm) by means of a rounded boattail on the nacelle. The exit of the new 14° primary flap was located at the largest plug diameter compatible with the smaller shroud and simulated a hinged iris primary operating at its minimum area with the capability of 60-percent area modulation.

The effect of nacelle shape on plug nozzle performance was also investigated with the tapered fairing shown on the lower part of Fig. 6. This fairing simulated a nacelle shape having a double conic juncture with a maximum diameter of 27.2 in. (69.1 cm).

Results

Auxiliary Inlet Ejector

A comparison of the flight data is made with unpublished cold-flow wind tunnel results in Fig. 7. In making this comparison it should be noted that this tunnel data between Mach 1.0 and 1.15 may not be representative of true isolated data since tunnel interference appeared to result in higher pressures on the external nozzle surfaces[8].

The data shown in the lower part of the figure are for 8°-16° and 10°-20° fixed-door configurations. With the primary nozzle at minimum afterburning and with the 8°-16° doors, little installation effect was observed. Between Mach numbers of 0.7 and 0.87, installed performance was slightly lower than isolated performance; the opposite trend occurred between Mach numbers of 0.87 and 0.95. The 8°-16° doors gave close to optimum performance for the installed nozzle. For the isolated nozzle, however, the highest performance occurred with the doors wide open (10°-20°). At Mach numbers below 0.93 the optimum installed performance was lower than the optimum isolated performance.

Figure 7 also shows the installation effect for maximum afterburner power setting with the doors closed. A favorable installation effect occurred between Mach numbers of 0.9 and 0.95 due to the lower boattail drag of the installed nozzle as was earlier observed for variable flap ejectors. From Mach number 0.95 to 1.0, a sharp increase occurred in the installed boattail drag resulting in a sharp decrease in installed performance. At Mach

number 1.0, the installed performance had decreased to a value such that little installation effect was observed.

The comparison of installed and isolated boattail pressure drags is presented in Fig. 8 for both minimum and maximum afterburning power settings. Installation of the nozzle caused a significant reduction in boattail drag especially at high subsonic Mach numbers (0.9 to 0.95) as the terminal shock moved toward the boattail and increased the pressures on the boattail. Above Mach number of 0.95, the terminal shock moved aft of the boattail and the decreased pressures on the boattail result in an abrupt increase in drag.

The effect of door position on performance was significantly different for the installed and isolated nozzles as can be seen in Fig. 9. The Mach 0.95 data is typical of the shape of the curves at all the subsonic speeds, but the differences between the installed and isolated data were greatest at this particular speed. Installed performance appeared to peak between the 5^{o}-10^{o} and 8^{o}-16^{o} door positions while the isolated performance continued to rise with increased door opening. It can be seen again, as in the previous figure, that the installed boatttail drag was reduced significantly. Since this improvement was larger (with the doors open) than the overall gain in gross thrust coefficient, it was apparently offset by poorer flow characteristics of the auxiliary inlets. The installed internal performance appeared to become relatively poorer as the doors were opened beyond their optimum position. For example, at the 10^{o}-20^{o} door position, the installed assembly had 6 counts lower boattail drag but comparable gross thrust coefficients. There was a considerable circumferential variation in static pressure and in the boundary-layer height and profile upstream of the auxiliary inlet doors. This resulted in a decrease in total pressure recovery through the auxiliary inlet doors when compared with isolated results. Also the pressure recovery varied from door to door, and measurements suggested that flow was actually exiting from some doors for all flight conditions shown.

A comparison of optimum installed performance using fixed doors with that obtained using the floating-door configuration is presented in Fig. 10. Results for both minimum and maximum afterburning power settings are shown. For both configurations, the doors floated to the position that gave close to optimum performance. For the maximum afterburning power setting, optimum performance occurred with the doors closed.

For these tests, the simulated trailing-edge flaps were fixed on the inner mechanical stops. Figure 11 shows the direction the trailing-edge flaps would move if allowed to float. With the minimum afterburner power setting, the flaps would move off the inner stops at Mach numbers of 0.9 or less because the internal flow was effectively separated from the walls resulting in high internal wall pressures relative to boattail pressures. As the Mach number increased above 0.9, the internal flow became effectively attached to the wall for some distance downstream of the shroud throat and the external terminal shock increased the boattail pressure. Consequently, the trailing-edge flaps would move to the inner stops.

For the maximum afterburner power setting, the flaps would be on the inner stops at Mach numbers from 0.9 to 0.98. The internal flow was effectively attached to the wall for some distance downstream of the shroud throat and the boattail drag was low resulting in low internal pressures relative to boattail pressures. As the Mach number increased, the nacelle terminal shock moved off the boattail and provided a sharp reduction in boattail pressures which would cause the flaps to move off the inner stops.

The principle purpose of the doors was to allow tertiary air to enter the ejector and separate the overexpanded primary jet, thereby improving performance. The floating doors were pressure actuated and moved according to the pressure difference across them. The position of each of the 16 doors is shown in Fig. 12 for the minimum afterburner power setting at a Mach number of 0.9. A considerable difference exists in the positions of the doors indicating a circumferential gradient in local external static pressure. A characteristic of the installation at high subsonic speeds is a high pressure region on the top of the nozzle assembly. There is also an accompanying distorted boundary layer on the bottom lower pressure portion of the nacelle. In general, the lower doors were almost completely closed whereas the top doors in the vicinity of the elevon trough were completely open. Even though the doors near the bottom of the ejector were almost closed, there was no significant circumferential variation in internal static pressures from top to bottom of the ejector.

Considerations such as the routing of electronic or hydraulic lines might dictate that some of the floating auxiliary inlet doors be blocked closed. Three door-blockage configurations were investigated at minimum afterburner power setting and are shown in Fig. 13. One configuration had the top three doors closed and another had the door under each elevon-nacelle juncture and the bottom door blocked close. These configurations resulted in about 19 percent of the door open area being blocked closed. The third configuration had two doors under each of the elevon-nacelle junctures and three doors at the bottom of the nozzle closed. It resulted in about 44 percent of the door open area being blocked closed. For all three configurations the unblocked doors were allowed to float under the influence of air loads.

The effect on nozzle performance is also shown in Fig. 13 for Mach numbers of 0.7 and 0.9. Blocking closed up to seven of the sixteen floating doors did not have a marked effect on installed performance. Apparently sufficient tertiary airflow was provided through the remainder of the doors.

In-flight movies were taken of the floating doors. The doors exhibited stable operation throughout the speed range.

Plug Nozzle

Installed performance of the plug nozzle is compared to unpublished data obtained in the 8- by 6-foot SWT with 0.34-scale isolated cold-flow models in Fig. 14. The

installation had little effect on performance at Mach numbers from 0.70 to 0.90. As Mach number was increased above Mach 0.90, the installed performance increased as the terminal shock moved into the nozzle region and peaked at a Mach number of 0.95. As Mach number was increased beyond 0.95, the terminal shock moved off the nacelle and a sharp drop in efficiency was measured which was considerably greater than measured in the isolated tests. The relatively low performance level at supersonic speeds of all the assemblies can be attributable to some degree to the small primary exit area relative to nacelle size. This small area resulted from the limitation to nonafterburning operation because of plug cooling considerations. The acceleration phase at low supersonic speeds with most aircraft would probably be done with afterburning and with corresponding larger primary area.

Comparison of the various component forces indicated that the major installation effect is caused by changes in the forces on the plug body. Fig. 15 compares isolated and installed pressure-integrated force data on the plug and also on the primary flap over the Mach range. Both forces reflect the same general trend as the installed nozzle performance.

The effect of the installation on the circumferential pressure distribution on the primary flap of the cylindrical nacelle assembly is shown in Fig. 16. The higher pressures on the top are typical of the distribution on all the assemblies tested. This circumferential pressure variation caused the secondary flow to exit asymmetrically in some instances with no flow being emitted near the top.

The performance of the cylindrical nacelle assembly is compared to the boattailed nacelle assembly in Fig. 17. The smaller exit diameter shroud (boattailed nacelle) exhibited slightly higher performance over the entire Mach range tested. A comparison of the component force differences between the boattailed and cylindrical assemblies is shown on the top part of the figure. It can be seen that the drag on the nacelle boattail is offset by higher pressure forces on the plug body and primary flap along with a larger secondary-flow exit momentum.

The effect of nacelle geometry variation from cylindrical to the tapered double-conic juncture is shown in Fig. 18. The presence of the tapered fairing resulted in a flow field that gave higher nozzle gross thrust subsonically but had essentially no effect above Mach 1.0. If the nozzle is charged for the drag on the aft conic surface of the tapered nacelle, performance was unaffected subsonically but significant deterioration was measured above Mach 1.0.

The effect of plug truncation on nozzle performance is shown in Fig. 19. A marked decrease in performance was measured with increasing amounts of plug truncation for the cylindrical nacelle assembly. The loss was more pronounced at supersonic speeds. However, the boattailed nacelle assembly showed no significant effect for the truncations tested. The primary jet expansion process on low-angle plug surfaces is a series of over and under expansions diminishing in intensity as they progress rearward. The number and intensity of these cycles was markedly less for the boattailed assembly. The data indicates that the degree of truncation possible, without adversely affecting nozzle performance, was sensitive to the configuration and Mach number.

Comparisons of the individual component forces which make up the total nozzle thrust-drag of the cylindrical nacelle assembly are shown in Fig. 20. The performance obtained with the load cell is compared to the summation of the pressure integrated component forces at the top of the figure and indicates good agreement. As can be seen for the component forces, the major force was the primary-flow exit momentum. The plug body was the only other component which contributed any thrust to the assembly and then only at subsonic speeds. The relatively low performance at supersonic speeds can be attributed primarily to the drag forces on the plug and primary flap.

Three high-response pressure transducers were used to measure dynamic pressures on the plug surface at 0° and 180° circumferential location, about half-way down the full-length plug and also in the base of the 50-percent truncated plug. The outputs were recorded on an analog tape recorder during each data scan. No evidence of unsteady pressure was detected.

Conclusions

Variations in the design of an auxiliary inlet ejector and of a plug nozzle were tested under the wing of an F-106B aircraft at Mach numbers from 0.7 to 1.3. The configurations simulated subsonic geometries of nozzles designed for high supersonic speeds (Mach ~ 2.8). Performance is compared with 0.34-scale isolated cold-flow results. The following results were obtained.

General

1. The installation caused a high pressure region on the top of the nozzle assemblies which affected the floating positions of the auxiliary doors and the pressure distribution on the surface of the plug.

2. No instabilities were obtained with floating auxiliary doors nor was there any oscillatory pressure variation on the surface of the plug.

Auxiliary Inlet Ejector

1. Favorable and unfavorable installation effects on peak performance were observed depending on the primary nozzle power setting. The installation caused a favorable reduction in boattail pressure drag, but this effect tended to be offset by an adverse effect on the door flow characteristics and internal performance. The net effect was slightly unfavorable at minimum afterburner power for Mach numbers less than 0.9, and a favorable effect occurred at maximum afterburner power for Mach numbers above 0.9.

2. The doors floated to the position that gave close to the optimum installed performance obtained with fixed

doors. Blocking closed seven of the 16 floating doors did not have a marked effect on performance.

Plug Nozzle

1. The installation had little effect on performance at Mach numbers from 0.70 to 0.90. At Mach 0.95 a significant improvement was measured as the terminal shock was in the vicinity of the nozzle and a large adverse effect occurred at Mach 1.0 after the terminal shock moved off the assembly.

2. Reducing the shroud-exit diameter by means of boattailing ahead of the shroud appeared to improve performance over the Mach range tested.

Symbols

AB	afterburner
C_p	static pressure coefficient
C_{M_T}	trailing-edge flap open moment coefficient
D	sum of nozzle external pressure and skin friction drags
D_β	nozzle boattail pressure drag
F	nozzle gross thrust
F_c	nozzle component force
F_{ip}	ideal thrust of primary flow
M_0	Mach number
P_8/p_0	nominal nozzle pressure ratio
x/ℓ	ratio of axial distance from primary-throat-to-overall plug length
$\omega\sqrt{\tau}$	secondary-to-primary corrected weight flow ratio

References

1. Nichols, M. R., "Aerodynamics of Airframe-Engine Integration of Supersonic Aircraft," TN D-3390, 1966, NASA, Hampton, Virginia.

2. Wilcox, F. A., Samanich, N. E., and Blaha, B. J., "Flight and Wind Tunnel Investigation of Installation Effects on Supersonic Cruise Exhaust Nozzles at Transonic Speed," paper 69-427, June 1969, AIAA, New York, N. Y.

3. Crabs, C. C., Mikkelson, D. C., and Boyer, E. O., "An Inflight Investigation of Airframe Effects on Propulsion System Performance at Transonic Speeds," presented at the 13th Annual Symposium of the Society of Experimental Test Pilots, Los Angeles, Calif., Sept. 25-27, 1969.

4. Blaha, B. J., "Effect of Underwing Engine Nacelle Shape and Location on Boattail Drag and Wing Pressures at Mach Numbers from 0.56 to 1.46," TM X-1979, 1970, NASA, Cleveland, Ohio.

5. Martlew, D. L., "Noise Associated with Shock Waves in Supersonic Jets," Aircraft Engine Noise and Sonic Boom, CP-42, May 1969, AGARD, Paris, France.

6. Burley, R. R. and Mansour, A. H., "Static Performance of an Auxiliary Inlet Ejector Nozzle Using an Afterburning Turbojet Gas Generator," TM X-1999, 1970, NASA, Cleveland, Ohio

7. Huntley, S. C. and Samanich, N. E., "Performance of a 10^o Conical Plug Nozzle Using a Turbojet Gas Generator," TM X-52570, 1969, NASA, Cleveland, Ohio.

8. Blaha, B. J. and Bresnahan, D. L., "Wind Tunnel Installation Effects on Isolated Afterbodies at Mach Numbers from 0.56 to 1.5," TM X-52581, 1969, NASA, Cleveland, Ohio.

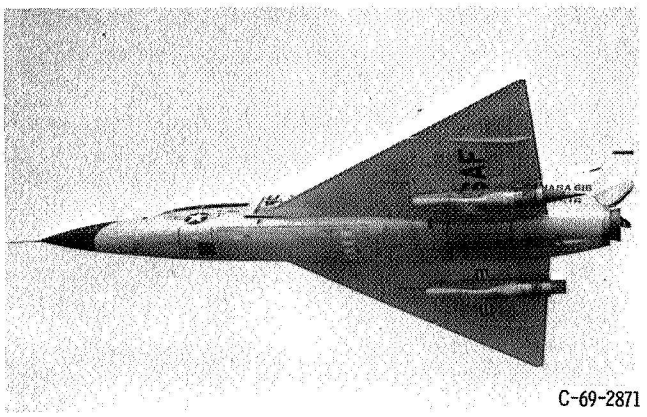

Figure 1. - Modified F-106B aircraft in flight.

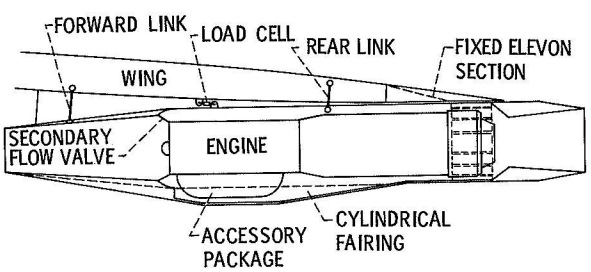

Figure 2. - Nacelle-engine installation.

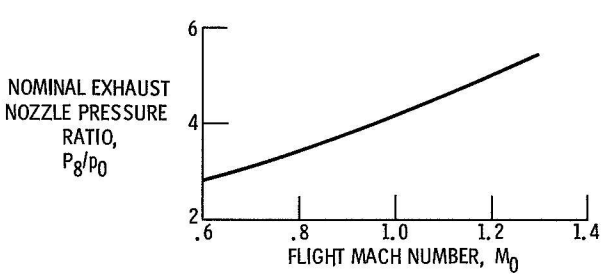

Figure 3. - Exhaust nozzle pressure ratio schedule.

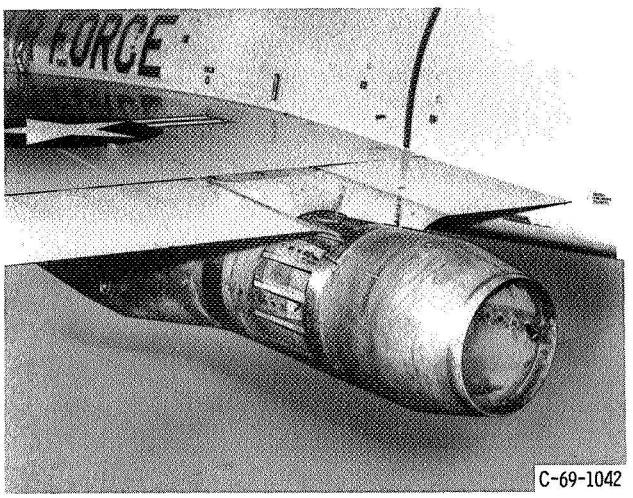

(a) Installed nozzle.

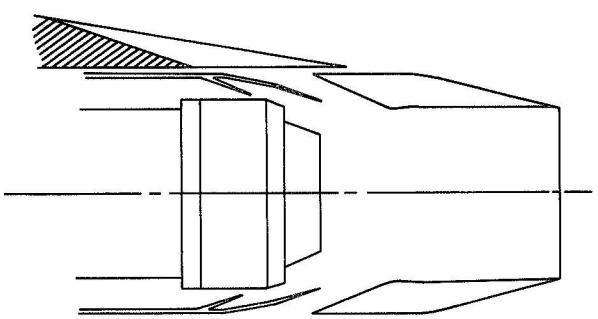

(b) Schematic.

Figure 4. - Auxiliary inlet ejector nozzle.

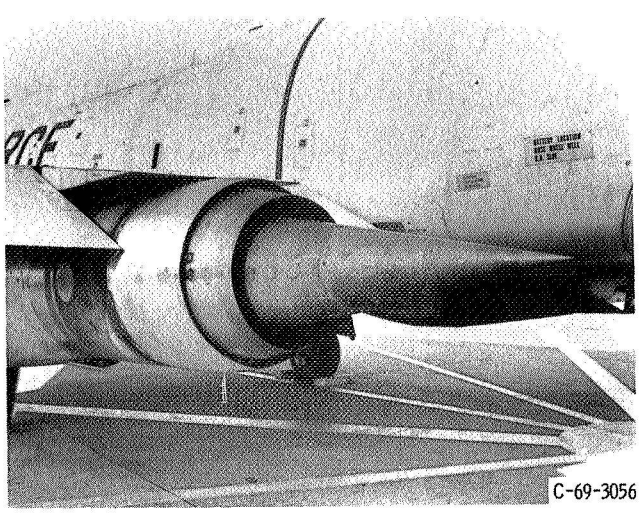

Figure 5. - Plug nozzle installation.

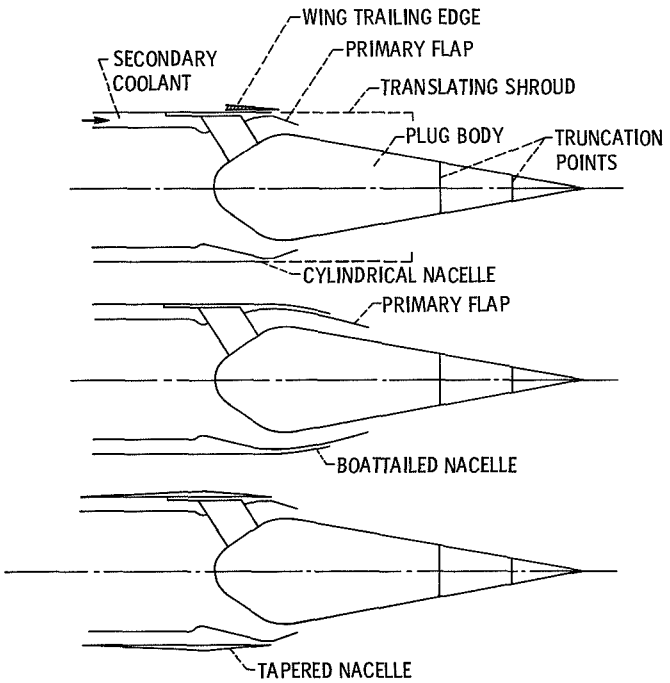

Figure 6. - Plug nozzle variations.

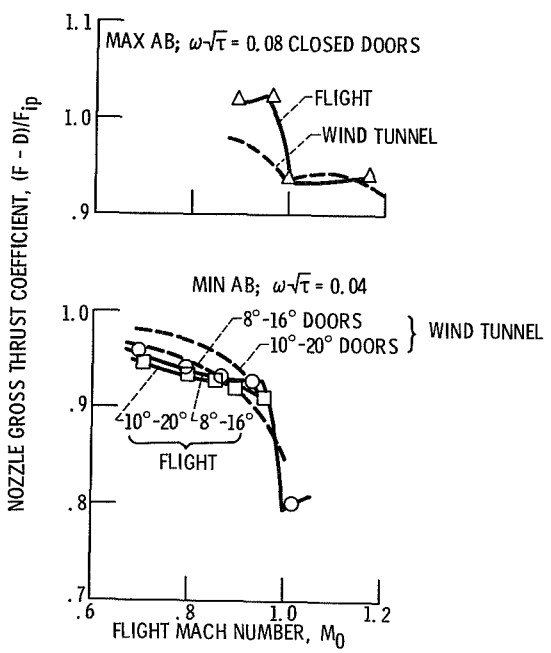

Figure 7. - Installation effect on AIE nozzle performance with fixed door configurations.

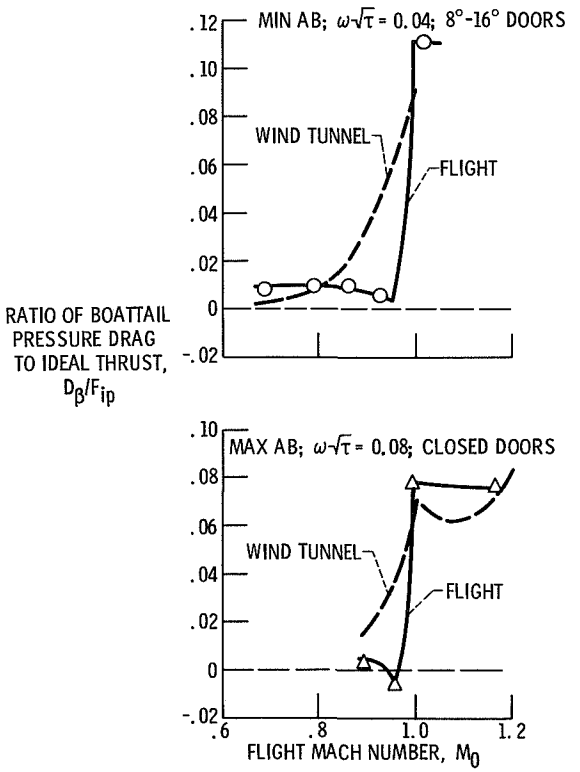

Figure 8. - Installation effect on AIE nozzle boattail drag with fixed door configurations.

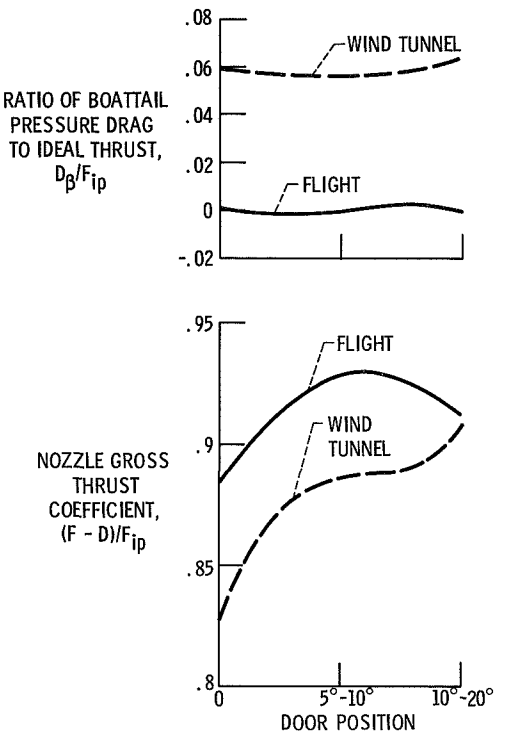

Figure 9. - Effect of door position. M_0 = 0.95; MIN AB; $\omega\sqrt{\tau}$ = 0.04.

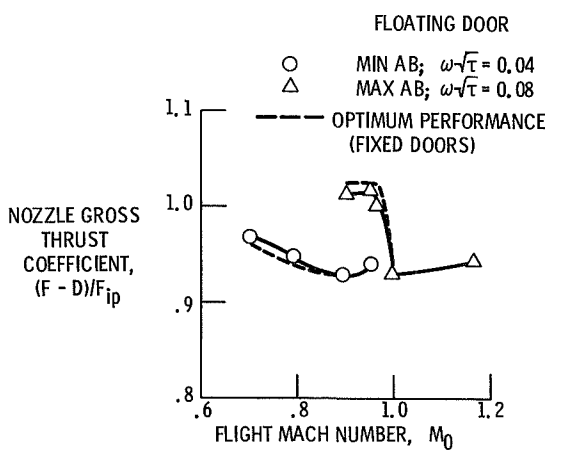

Figure 10. - Installed performance of floating door configuration compared with optimum fixed door performance.

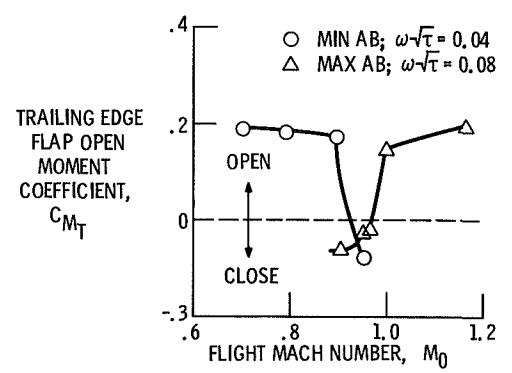

Figure 11. - Effect of Mach number on trailing edge flap moment coefficient; floating door configuration.

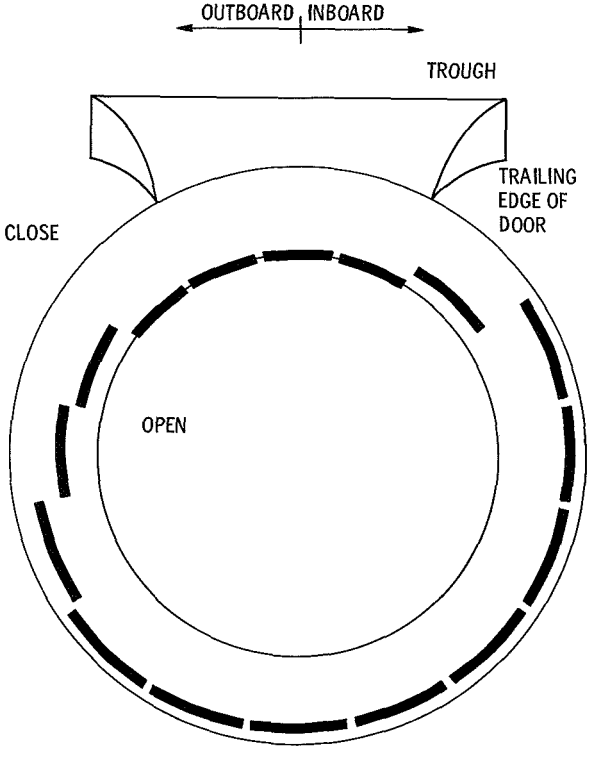

Figure 12. - Positions of the floating doors. $M_0 = 0.9$; $\omega\sqrt{\tau} = 0.04$; MIN AB.

PERCENT CLOSED	DOORS CLOSED
18.75	3, 9, 15
18.75	1, 2, 16
43.75	3, 4, 8, 9, 10, 14, 15
100	ALL

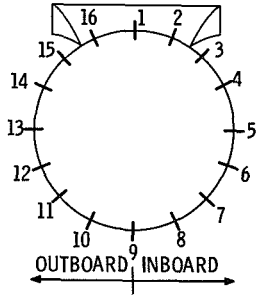

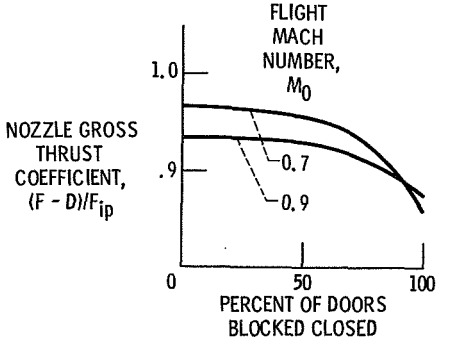

Figure 13. - Effect of door blockage on nozzle performance. MIN AB; $\omega\sqrt{\tau} = 0.04$.

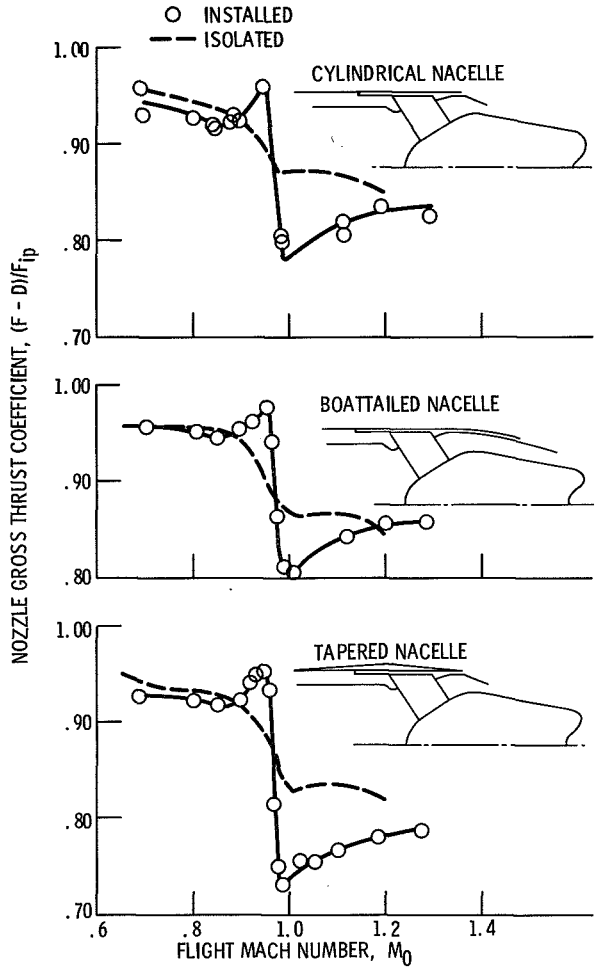

Figure 14. - Installation effect on plug nozzle performance.

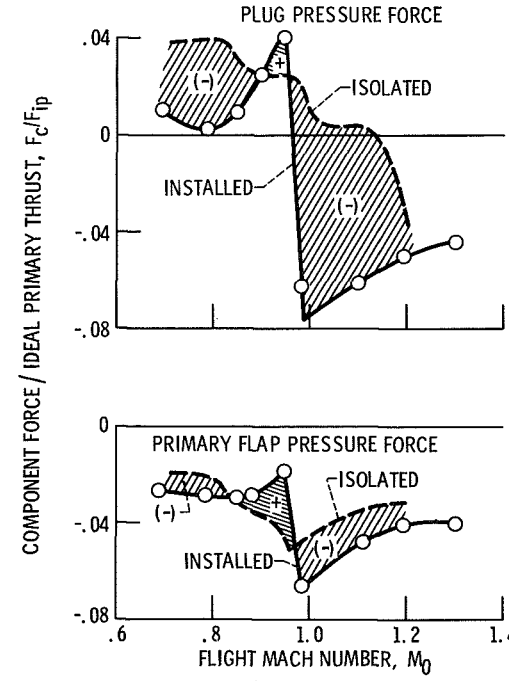

Figure 15. - Plug and primary flap pressure force, isolated and installed (cylindrical nacelle).

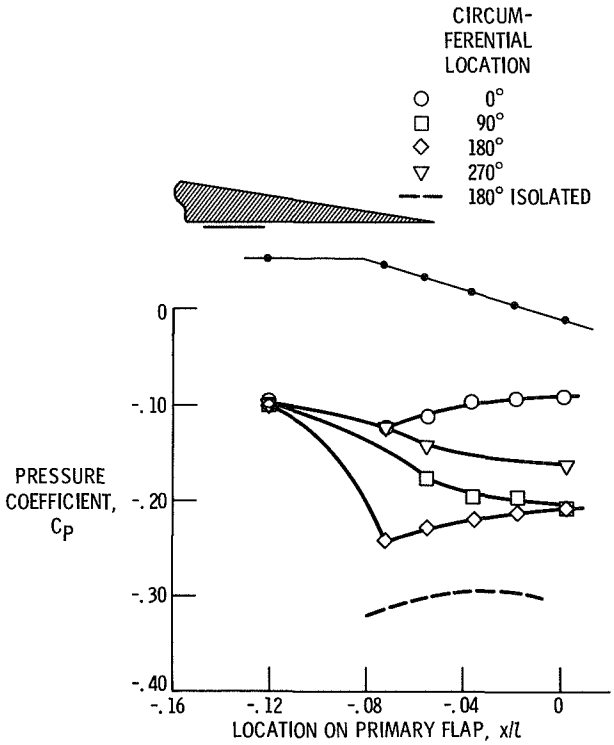

Figure 16. - Circumferential pressure variation on primary flap of cylindrical nacelle assembly.

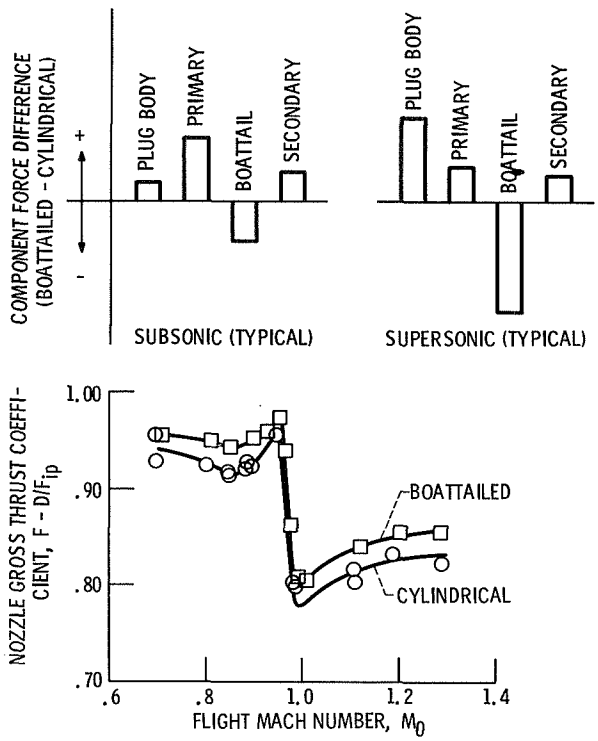

Figure 17. - Comparison of boattailed and cylindrical nacelle performance and component forces.

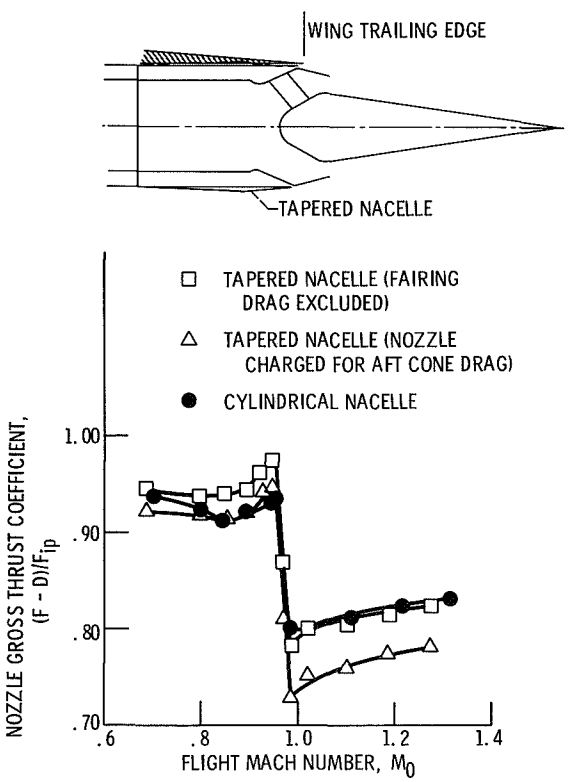

Figure 18. - Effect of nacelle geometry on plug nozzle performance.

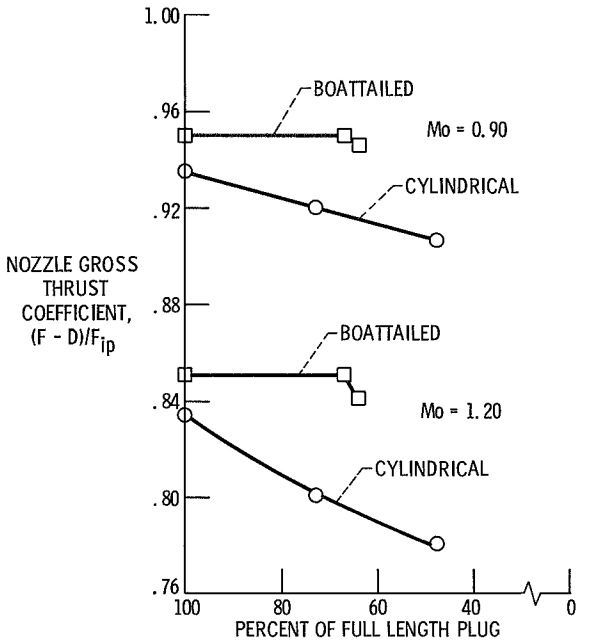

Figure 19. - Effect of plug truncation on nozzle performance.

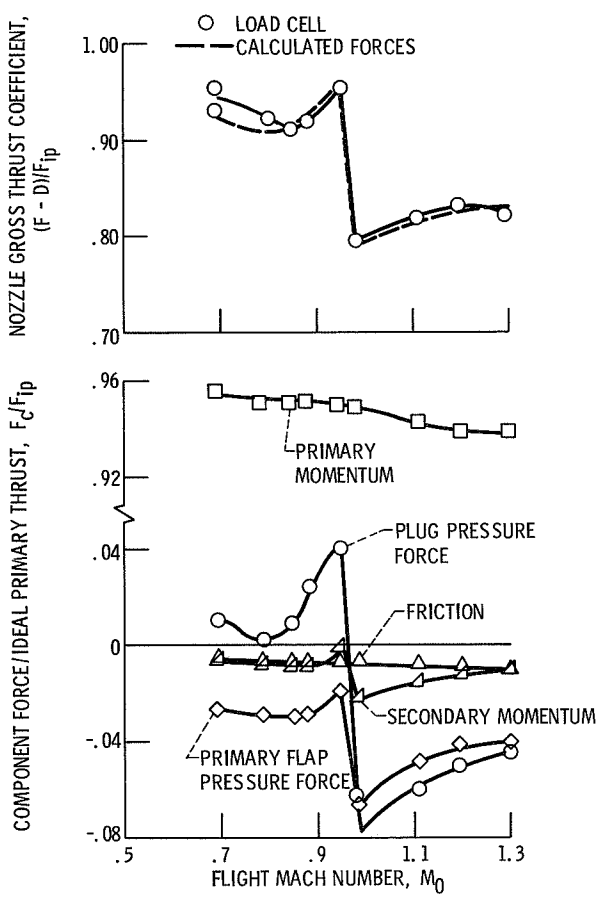

Figure 20. - Component force breakdown 100 percent plug, cylindrical nacelle, $\omega\sqrt{\tau} = 0.034$.